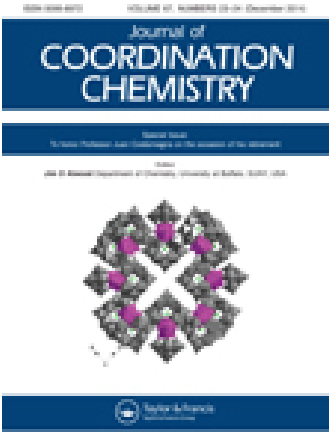

Journal of Coordination Chemistry
Publication details, including instructions for authors and subscription information:
http://www.tandfonline.com/loi/gcoo20

Preparation, spectroscopic, and electrochemical characterization of metal(II) complexes with Schiff base ligands derived from chitosan: correlations of redox potentials with Hammett parameters

Claudia A. Caro[a], Gerardo Cabello[a], Esteban Landaeta[b], Jerónimo Pérez[a], Miguelina González[a], José H. Zagal[c] & Luis Lillo[a]

[a] Facultad de Ciencias, Departamento de Ciencias Básicas, Universidad del Bío-Bío, Chillán, Chile

[b] Facultad de Química, Departamento de Química Inorgánica 2, Pontificia Universidad Católica de Chile, Santiago, Chile

[c] Facultad de Química y Biología, Departamento de Química de los Materiales, Universidad de Santiago de Chile, Santiago, Chile

To cite this article: Claudia A. Caro, Gerardo Cabello, Esteban Landaeta, Jerónimo Pérez, Miguelina González, José H. Zagal & Luis Lillo (2014) Preparation, spectroscopic, and electrochemical characterization of metal(II) complexes with Schiff base ligands derived from chitosan: correlations of redox potentials with Hammett parameters, Journal of Coordination Chemistry, 67:23-24, 4114-4124, DOI: 10.1080/00958972.2014.977271

To link to this article: http://dx.doi.org/10.1080/00958972.2014.977271

Journal of Coordination Chemistry, 2014
Vol. 67, Nos. 23–24, 4114–4124, http://dx.doi.org/10.1080/00958972.2014.977271

Preparation, spectroscopic, and electrochemical characterization of metal(II) complexes with Schiff base ligands derived from chitosan: correlations of redox potentials with Hammett parameters

CLAUDIA A. CARO†, GERARDO CABELLO†, ESTEBAN LANDAETA‡, JERÓNIMO PÉREZ†, MIGUELINA GONZÁLEZ†, JOSÉ H. ZAGAL§ and LUIS LILLO*†

†Facultad de Ciencias, Departamento de Ciencias Básicas, Universidad del Bío-Bío, Chillán, Chile
‡Facultad de Química, Departamento de Química Inorgánica 2, Pontificia Universidad Católica de Chile, Santiago, Chile
§Facultad de Química y Biología, Departamento de Química de los Materiales, Universidad de Santiago de Chile, Santiago, Chile

(*Received 27 August 2014; accepted 7 October 2014*)

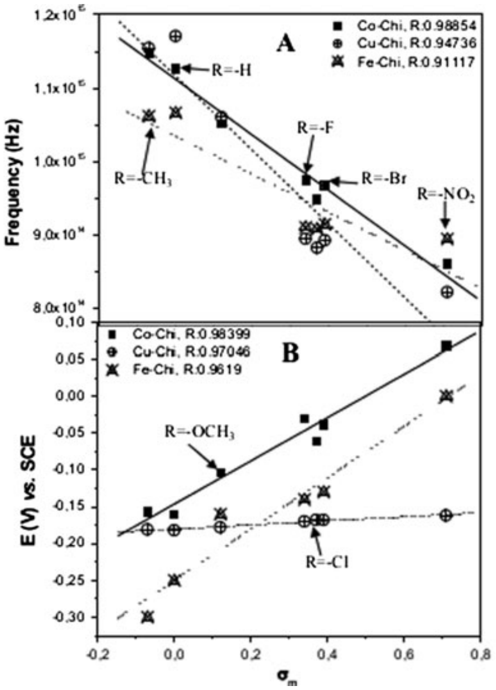

---

*Corresponding author. Email: llillo@ubiobio.cl

The chitosan–(Fe(II), Co(II), and Cu(II)) complexes were prepared by mixing chitosan (Chi) powder with a salicylaldehyde (Sal, 5-hydrogen (–H)) and their 5-bromo (–Br), 5-chloro (–Cl), 5-methoxy (–OCH_3), 5-fluoro (–F), 5-methyl (–CH_3), and 5-nitro (–NO_2) derivatives (groups R) and mixing these with $FeCl_2$ and $CuCl_2$ in ethanol and with $Co(CH_3COO)_2$ solutions in butanol at 80 °C over 8 h in heterogeneous phase, followed by extraction with ethanol and butanol, respectively. The complexes were characterized by FTIR and UV–vis spectroscopy, elemental analysis, and cyclic voltammetry. A linear correlation between the metal formal potential *versus* the Hammett parameters of the substituents was observed. The electron-withdrawing groups shift the redox potential to positive values, as a result of lowering the energy of the highest occupied molecular orbital. The formal potential was used as a measurement for the driving force of chitosan complexes for redox reactions.

Keywords: Chitosan; Schiff base complexes; Cyclic voltammetry; Hammett correlations

1. Introduction

Chitosan, the linear β-(1→4)-linked polysaccharide of 2-amino-2-deoxy-D-glucose repeating units, can be isolated from chitin. The natural polysaccharide of chitosan and its derivatives have diverse potential applications in biotechnology, biomedicine [1, 2], food ingredients, and cosmetics [3] because of their properties, such as hydrophilicity, biocompatibility, biodegradability, anti-bacterial properties [4–6], and remarkable affinity with many biomacromolecules [7]. Some derivatives have been characterized but their electrochemical characterization is limited; so, it is of interest to carry out an investigation on the development of biosensors and biocatalysts using these systems [8, 9].

In particular, chitin and chitosan, two low-cost natural materials, have been used for the adsorption of metal ions, dyes, and proteins [10–14]. The principal studies on chitosan and ions have been focused on the adsorption of metal ions in aqueous solutions like Cu(II), Zn (II), and Pb(II) [15]. Recently, a study about chitosan-based magnetic nanoadsorbents using Fe_3O_4 nanoparticles as cores and chitosan as ionic exchange groups was carried out, showing chitosan to be efficient for the fast adsorption of Cu(II) ions and acid dyes [16, 17]. The recovery of Co(II) ions from aqueous solutions using the magnetic chitosan nanoadsorbent has also been examined [18]. Electrochemical studies have shown some new applications of these kinds of complexes, like metal ion adsorption and as electrocatalysts for some reactions. Huang *et al.* [19] carried out a study on chitosan biopolymer films with a heme group, obtaining redox peaks located at potentials that are typical of the Fe(III)/II) redox couple. Oxidation of nitrite was studied with carboxylated chitosan over glassy carbon (GC) electrodes with high activity [20]. It is essential to characterize the intrinsic redox behavior of these polymers before examining their catalytic activity for an electron transfer reaction. The correlations between the metal-centered redox potential and Hammett parameters of ligand substituents clearly showed the influence of the electronic effect of substituent groups on the electron density located at the metal, affecting their redox potentials and catalytic activity. There are publications about other systems with linear correlations between the catalytic activity of some complexes, like metal phthalocyanines and their redox potential [21–23]. In these correlations, the rate constant decreases or increases, depending on the reaction, with an increase in the driving force of the catalyst (redox potential).

The main objective of the present work was to synthesize chitosan–M(II) complexes (M = Co, Cu, and Fe). Spectroscopic, electroanalytical, and UV–vis studies were carried out and discussed in order to assign the metal redox peaks for these complexes. The relationship between frequency and voltammetric peaks with Hammett parameters were analyzed and compared with the information for the chitosan Schiff bases without metal ions [24]. This allowed an understanding of the mechanism of charge transfer of these complexes.

2. Experimental

2.1. *Materials*

Chitosan was purchased from Sigma Chemical Co., average MW: 1.11 × 10^6 Dalton [25]. $Fe(Cl)_2$, $CuCl_2$, $Co(CH_3COO)_2$, salicylaldehyde, and derivatives with different electron-donating and electron-withdrawing groups (5-bromine, 5-chlorine, 5-methoxy, 5-fluorine, 5-methyl, and 5-nitro) were supplied by Aldrich Chemical Co. The analytical grade electrolytes (H_2SO_4, KCl, KH_2PO_3, and Na_2HPO_3) were obtained from Merck.

2.2. *Elemental analyses and FTIR spectroscopy*

Elemental analyses were performed in a FISIONS-EA 1108 analyzer. The metal content was determined by atomic absorption using Perkin Elmer 2380 equipment. The native chitosan and derivatives were characterized by FTIR in a FTIR-4100 Jasco spectrophotometer. All spectra were recorded with an accumulation of 64 scans and resolution of 4 cm^{-1} from 4000 to 200 cm^{-1}. For IR spectra, the samples (2.0 mg) were dried for 24 h at 60 °C under reduced pressure and were mechanically mixed with 20 mg of KBr. Derivation, including the Savitzky–Golay algorithm with 25 smoothing points, was performed using the OPUS/I.R. version 1.4 software incorporated into the hardware of the instrument [26, 27]. The degree of *N*-acetylation of commercial chitosan determined by FTIR spectroscopy was approximately 30% [28].

2.3. *UV–vis spectroscopy*

UV–vis spectra were obtained with 1 nm resolution in a Perkin Elmer Model Lambda 25 UV–vis spectrophotometer. These spectra were measured in aqueous solutions for Cu(II) and Co(II) complexes and in DMSO for Fe(II) complexes.

2.4. *Electroanalytical measurements*

Measurements were conducted on an electrochemical analyzer potentiostat/galvanostat Model 600 D Series of CH Instruments. The working electrode (Pine Instruments) was a GC disk of 0.196 cm^2 geometrical area. The electrode was cleaned in 0.5 M sulfuric acid at positive and negative constant potentials. The cell was purged for 240 s and then the electrode was polished using 1200 and 4000 grit emery paper followed by ultrasonic treatment in 0.5 M sulfuric acid. A saturated calomel electrode was used as reference and the auxiliary electrode was a platinum (99.99%, Pine Instruments) spiral wire exposing an area of 14 cm^2. The electrolytes were prepared from deionized, double-distilled water, and deaerated with ultra-pure N_2.

2.5. *Synthesis of chitosan–M(II) complexes*

The Schiff bases were synthesized by condensation of a suspension of chitosan (0.1 g, 9.01×10^{-5} mM) and salicylaldehyde derivatives (0.14 g, 1.15 mM) in 15 mL of methanol. The salicylaldehyde derivatives are: 2-hydroxy-5-methoxybenzaldehyde (*R* = $-OCH_3$), 5-hydroxy-5-nitrobenzaldehyde (*R* = –NO2), 5-hydroxy-5-methylbenzaldehyde (*R* = $-CH_3$), 5-hydroxy-5-chlorobenzaldehyde (*R* = –Cl), 5-hydroxy-5-fluorobenzaldehyde (*R* = –F), and 5-hydroxy-5-bromobenzaldehyde (*R* = –Br). These mixtures were refluxed with stirring for 16 h at 60 °C. The solid was filtered off, washed with methanol, and dried at 30 °C. The dried material was extracted in a Soxhlet for 10 h with methanol, washed with diethyl ether, and dried in vacuum to give a yellow solid (73.5% yield). Chitosan–M(II) complexes were prepared by mixing Schiff base powders with 0.11 g (0.87 mM) $FeCl_2$, 0.14 (1.04 mM) $CuCl_2$, and with 0.058 g (0.23 mM) $Co(CH_3COO)_2 \cdot 4H_2O$ solutions. These mixtures were refluxed in butanol with stirring for 8 h at 80 °C. The solids were filtered off, washed with ethanol, and dried at 30 °C (see figure 1) [26–29].

3. Results and discussion

3.1. *Elemental analysis*

The elemental analysis results of the Schiff bases and the content of metal in the complexes are presented in table 1. The results are quite different from those expected for a 100% degree of substitution, suggesting that this process was not complete (degree of *N*-acetylation was 30%). This means that the free amino groups (70%) of chitosan were fully substituted obtaining the corresponding Schiff base, making it unnecessary to change the amino groups [28]. The degree of substitution calculation was done considering the experimental C/N ratio. The calculated percentages using the experimental data are consistent with Schiff base formation. However, the presence of salicylaldehyde and its derivatives caused an increase in the carbon and hydrogen content in the resulting materials compared to chitosan.

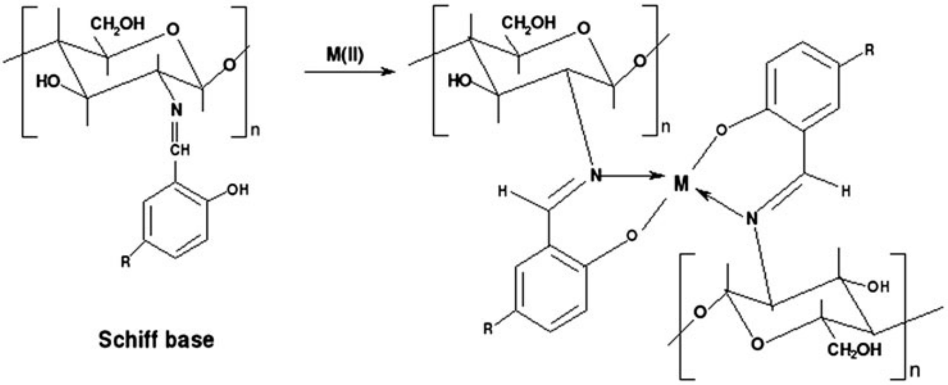

Figure 1. Reaction scheme of the Schiff base with substituted groups (where *R* = –H, $-CH_3$, –Cl, $-NO_2$, –F, –Br, and $-OCH_3$) and the metal (M = Co, Cu, and Fe).

Table 1. Elemental analysis of chitosan, Schiff bases, and complexes.

	Element (%)				Metal (%)		
Sample	C	H	N	C/N	Fe	Cu	Co
Chi	43.8	6.47	7.94	5.52	–	–	–
–H	53.4	5.36	5.72	9.33	6.82	7.58	7.23
–Cl	49.3	4.15	4.51	10.9	4.22	6.46	6.03
–F	47.4	4.12	4.46	10.6	3.55	8.32	8.23
$–NO_2$	47.5	4.13	8.51	5.58	3.71	3.35	3.45
$CH_3O–$	55.3	5.48	4.46	12.4	5.71	8.45	8.33
–Br	48.2	4.23	4.67	10.3	4.30	8.01	8.41
$–CH_3$	56.6	5.67	5.23	10.8	5.69	7.59	7.46

Note: Chi (chitosan); Schiff base (–H, –Cl, –F, $–NO_2$, $CH_3O–$, –Br, and $–CH_3$).

3.2. *FTIR spectroscopy*

The FTIR spectra (table 2) of Schiff bases showed high absorption levels between 1631.5 and 1640.9 cm^{-1} attributed to the C=N stretch characteristic of the imino group and a signal at 1573.4 cm^{-1} (C=C stretching aromatic ring) and 1496.4 cm^{-1} (C=C deformation of aromatic ring) [24, 28]. The second derivative FTIR spectra of chitosan complexes of the Schiff bases showed a tendency to lower wave numbers in the C=N absorption relative to the free ligand, indicating coordination of the nitrogen of the Schiff bases to the metal ion (see figure 2) [30]. Costamagna and coworkers [26, 29, 30] found that the frequencies showed a shift in the C=N absorption relative to the free ligand spectrum indicating coordination of the nitrogen to copper and nickel ion. Its appearance indicates that the alcoholic groups of the sugar moiety do not participate in coordination to the metal. Two new bands in relation to the free ligand in the FTIR spectrum assigned to Co–O (385.4 cm^{-1}) and to Co–N (267.3 cm^{-1}) stretches corroborate the formation of the Co(II) complex. Similar signals were observed for Cu(II) and Fe(II) complexes.

3.3. *UV–vis spectral studies*

Absorption spectra of chitosan–Co(II) complexes dissolved in water are shown in figure 3(A). All transitions below 400 nm are assigned to intra-ligand charge transfer, attributed to the benzene ring transition ($\pi \rightarrow \pi^*$) at lower wavelengths, and the second transition

Table 2. IR bands of the imino group of the Schiff bases and of the complexes.

	Infrared (cm^{-1})				
Sample	δ_{NH} (amine)	$\nu_{C=N}$ (imine)	Fe(II) complexes $\nu_{C=N}$ (imine)	Cu(II) complexes $\nu_{C=N}$ (imine)	Co(II) complexes $\nu_{C=N}$ (imine)
Chi	1594.9	Absent	Absent	Absent	Absent
–H	nd	1639.3	1632.4	1623.3	1630.9
–Cl	nd	1635.8	1633.4	1628.1	1627.8
–F	nd	1635.8	1629.7	1626.5	1629.2
$–NO_2$	nd	1640.9	1625.2	1632.9	1630.9
$CH_3O–$	nd	1635.8	1630.7	1636.1	1637.1
–Br	nd	1631.5	1620.7	1621.7	1619.5
$–CH_3$	nd	1637.1	1626.7	1629.7	1630.0

Note: Chi (chitosan); Schiff base (–H, –Cl, –F, $–NO_2$, $CH_3O–$, –Br, and $–CH_3$); nd, not detected; ν, stretching.

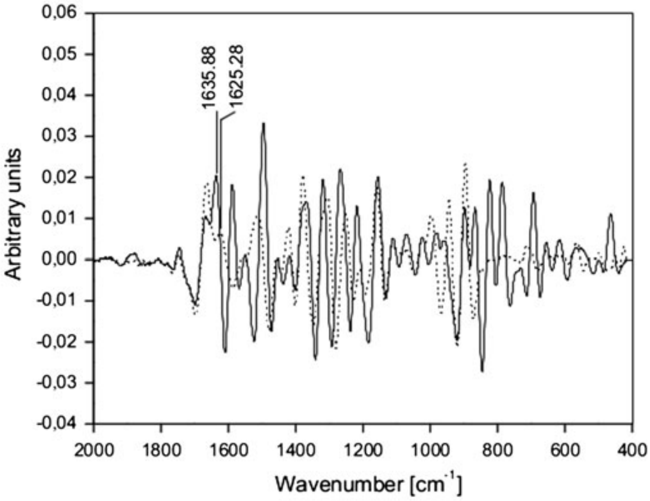

Figure 2. Second derivative FTIR spectra from ~2000 to 400 cm^{-1} of: (—) Schiff base when $R = -F$. (—) Chitosan Fe(II) complex when $R = -F$.

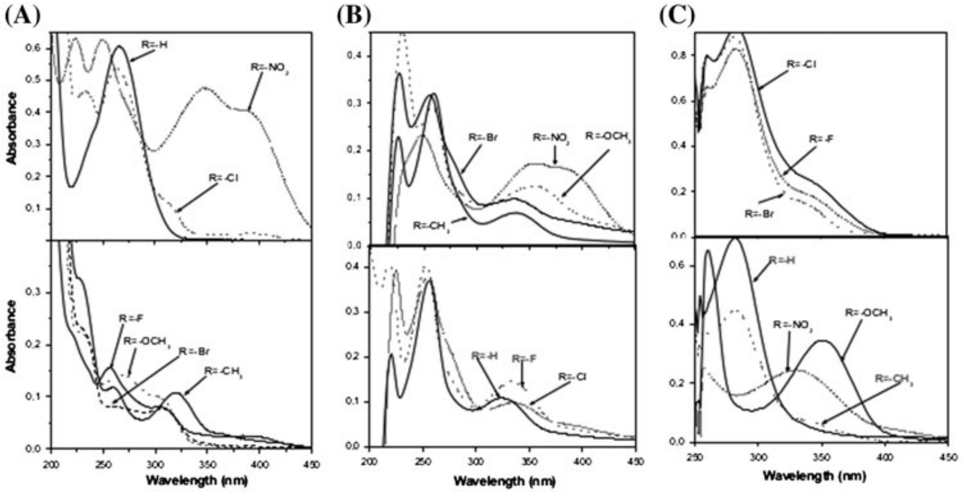

Figure 3. UV–vis spectra of: (A) Cobalt–chitosan complexes in water. (B) Copper–chitosan complexes in water. (C) Iron–chitosan complexes in DMSO.

assigned to $-C_6H_5-OH$ ($n \rightarrow \pi^*$) [24]. For all chitosan–Co(II) complexes, the electronic transitions moved to higher energies and for some complexes, other signals appear when compared to Schiff bases [24]. For example, when $R = -Cl$, two new signals appear at 270 and 390 nm, and when $R = -CH_3$ and $-OCH_3$, a new signal appears for both complexes at 260 and 270 nm, respectively. The absorption spectra of chitosan–Cu(II) complexes dissolved in water are shown in figure 3(B). For all chitosan–Cu(II) complexes, the electronic transitions shift to lower energies except when $R = NO_2$ which presents a Hammett parameter of 0.71 in the meta position (more electron withdrawing). The rest of the chitosan–Cu

(II) complexes show two new signals between 200 and 300 nm which are absent with the Schiff bases [24]. When compared with the transition shown by the Schiff bases, all the electronic transitions of the chitosan–Fe(II) complexes tended to show higher energies, except for the complex with *R* = –OCH_3. The methoxy group does not promote the intraligand charge transfer because of its electron donor properties. When *R* = –F, –Br, –Cl, and –CH_3 two new signals at 350 nm were displaced from ~420 nm [see figure 3(C)]. The complexes were dissolved in DMSO and the spectra were measured in the 200–1000 nm range. The complexes are square-planar as suggested by the d–d transition shown as weak band near 590 nm that probably is under the intense band at around 470 nm in the complexes. Similar results were published by Costamagna *et al.* for poly-D-galactosamine complexes of Cu(II) and Ni(II) [26, 29].

3.4. *Electrochemical studies*

Figure 4 depicts a series of cyclic voltammograms illustrating the potentiodynamic response of different substituted chitosan–M(II) complexes adsorbed on GC. Cyclic voltammograms

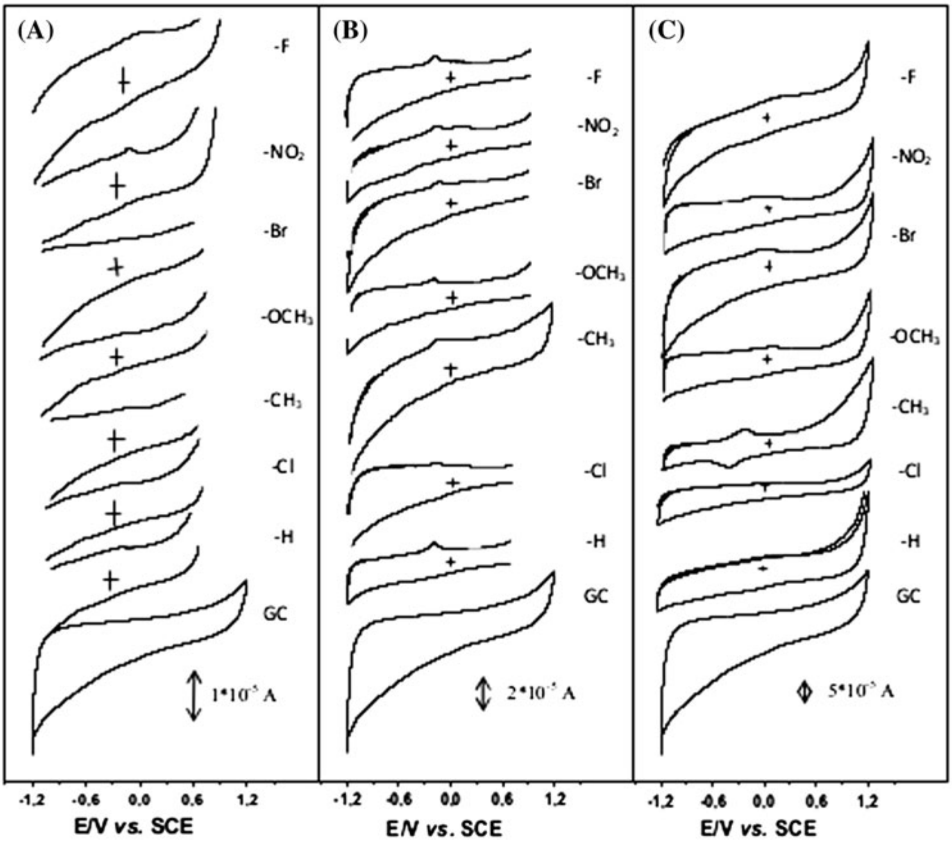

Figure 4. Cyclic voltammograms of: (A) Cobalt–chitosan complexes adsorbed on a GC surface. (B) Copper–chitosan complexes adsorbed on a GC surface. (C) Iron–chitosan complexes adsorbed on a GC on surface. Phosphate buffer pH 7.3. N_2 saturated. Scan rate, 0.1 V s^{-1}.

were obtained in KH_2PO_4–Na_2HPO_4 buffer (pH 7.26). Intrinsic parameters of the redox couple or redox peak of adsorbed catalyst were determined using fast-scan cyclic voltammetry (scan rates up to 0.1 V s^{-1}). The chitosan–Co(II) complexes show one redox couple that corresponds to the Co(III)/II) process [24]. For example, the chitosan–Co(II) complex [figure 4(A)] when $R = H$ has an anodic peak at ca. 0.099 V and a cathodic peak at −0.106 V, attributed to the Co(III)/(II) redox process that shows some irreversibility. Similar processes are observed for the chitosan–Co(II) complex when R = –F, –Br, $–OCH_3$, and $–CH_3$. Another weak signal at −0.63 and −0.65 V appears in the cyclic voltammograms when R = –Cl and R = $–NO_2$, respectively, attributed to the Co(III)/(II) redox process.

The chitosan–Cu(II) complex has an irreversible peak at ca. −0.2 V attributed to a process centered on the metal, i.e. Cu(II)/(I); this is shown in figure 4(B). In this case, the irreversibility can be attributed to the fact that the redox process involves a change in geometry (Cu(I) tetrahedral)/Cu(II) planar) that may conceal the redox process. For example, the chitosan–Cu(II) complex when R = H has an anodic peak at ca. −0.18 V. Similar processes are observed in the chitosan–Cu(II) complex when R = $–OCH_3$. The chitosan–Cu(II) complex with R = –F, –Br, –Cl, $–NO_2$, and $–CH_3$ showed a broad cathodic wave at ca. −0.23, −0.25, −0.16, −0.51, and −0.21 V, respectively, that can be assigned to the Cu(II)/(I) redox process.

Similar patterns are observed in cyclic voltammograms of chitosan–Fe(II) complexes and cyclic voltammograms of chitosan–Co(II) [figure 4(C)]. All chitosan–Fe(II) complexes, excluding those where R = –Cl, have a redox couple. When R = –F, $–OCH_3$, and –H, this couple appears at ca. −0.12 V (cathodic peak) and 0.09 V (anodic peak), while the others showed this redox process at −0.3/−0.15 V when R = $–NO_2$, −0.31/−0.12 V when R = –Br, and −0.4/−0.2 V when R = $–CH_3$ (cathodic/anodic order). The difference between cathodic and anodic peaks remains constant and is ~ −0.2 V.

Cyclic voltammograms of Co and Fe phthalocyanines, adsorbed on ordinary glassy graphite and recorded in oxygen-free 0.1 M NaOH, showed M(II)/(I) couples at ca. −0.65 and −0.68 V, respectively, and the M(III)/(II) couples appear at ca. 0.5 and −0.15 V, respectively [31]. Cyclic voltammograms of cobalt and iron phthalocyanines recorded in oxygen free pH 7.3 showed M(II)/(I) couples at ca. −0.55 and −0.6 V, respectively, and the M(III)/(II) couples appear at ca. 0.45 and 0.2 V, respectively [32]. In these cases, at pH 12.4, the couple Co(II)/(I) is at ca. −0.53 V and the couple Fe(II)/(I) is at ca. −0.79 V (this is not observed at pH 7.3), and couple Co(III)/(II) at basic pH change compared with voltammogram was obtained at pH 7.3. The redox peaks were assigned according to these data. It was concluded that the metal ions are coordinated and have redox activity.

All complexes studied showed a displacement of the reduction process to more negative potentials. That means that the oxidized compounds are adsorbed more effectively than the reduced compounds. Then, $\beta_{ox} > \beta_{red}$, where β is the relation between surface concentration of chitosan complexes on the electrode surface and surface concentration of saturation on the electrode surface, and this is related with the Gibbs free energy function ($\Delta G°$) by the expression $\beta_i = e^{-\Delta G°/RT}$ according to a Langmuir adsorption isotherm. A larger β_{ox} involves a negative $\Delta G°$ and a spontaneous adsorption of the oxidized compound [32].

Our group has studied the correlations between the redox potentials and frequencies of Schiff bases of chitosan and the electronic properties of substituents on the ligand. This has been done with the complexes confined on the surface of GC electrodes using Hammett substituent constants, and many linear correlations have been found [24]. Figure 5(A) illustrates a plot of frequency *versus* the Hammett parameters σ_m of the groups reported in the literature [33]. The electron-withdrawing groups cause a displacement to lower frequencies. Figure 5(B) illustrates a plot of M(II)/(I) (M = Co, Cu, and Fe) formal potentials $E°$ *versus*

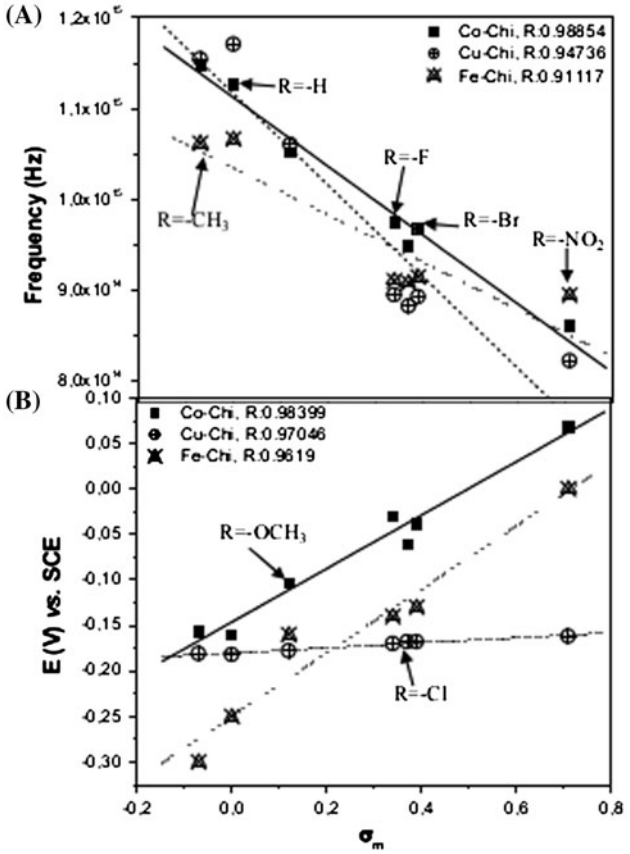

Figure 5. (A) Variation of the frequency *vs.* the Hammett parameters of the substituents. (B) Variation of peak potential *vs.* the parameters of the substituents.

the Hammett parameters σ_m of the groups. The plot exhibits three straight lines which essentially show that the M(II)/M(I) process is sensitive to the effect of the substituents, considering that 70% of chitosan forms the Schiff base and the relation between the Schiff base and the metal is 2 : 1.

Electron-withdrawing groups shift redox potentials to more positives values, and the opposite is true for electron-donating groups, compared to M–Chi. Figure 5(A) indicates that these groups modulate the electron density on the M center. That is crucial for electrocatalytic processes mediated by these complexes, because these may affect the M(II)/(I) formal potential and the binding properties of the M center, which are vital in catalytic processes as they involve the binding of a target molecule to the metal center. It is also probable that these groups affect the energy of the frontier orbital involved in the redox process. As the electron-withdrawing power of the groups increases, it should cause a lowering of the highest occupied molecular orbital (HOMO) energy [34]. Then, it becomes more difficult to remove an electron from this orbital and that is reflected in a more positive redox potential. The energy of the HOMO also affects the affinity of the metal to bind an extra planar ligand, since the energy of the bond to be formed depends on the energies of the orbitals involved [35, 36].

4. Conclusion

We have prepared chitosan complexes by the reaction of Schiff bases with different central metals (M = Fe, Co, and Cu). The chitosan complexes were characterized by FTIR spectroscopy, UV–vis spectrophotometry, and cyclic voltammetry. The principal charge transfers may be attributed to processes of reduction that occur in the imine group (–C=N) and oxidation of OH– groups which are displaced to higher energies with the metal incorporation. The presence of chitosan complexes on the GC electrode has been demonstrated, together with the fact that the oxidized compounds are adsorbed more effectively than the reduced compounds for these complexes. Cu complexes exhibit a redox process centered at the metal and assigned to Cu(II)/(I). This process shows some degree of irreversibility, as expected, as a result of the geometry change from Cu(II) having a planar configuration to Cu(I) having a tetrahedral configuration. In contrast, Fe and Co complexes exhibit both M (II)/(I) and M(III)/(II) couples. There is a linear correlation between the frequency and the M(II)/(I) formal potential $E^{\circ,\prime}$ which also *versus* the sum of the Hammett parameters of substituents on the ligand. The electron-withdrawing groups cause a shift of the UV–vis bands to lower energies, and also a shift of the formal potentials to higher values as a result of the lowering of the energy of the HOMO. The formal potential can also be used as a measurement of the driving force of chitosan complexes anchored on electrode surfaces for the promotion of catalytic reactions [21–23].

Acknowledgements

The authors are grateful for the financial support from FONDECYT Projects N° 1120164 and Nº 1140199 and to the Dirección de Investigación de la Universidad del Bío-Bío (Grant DIUBB 142209 4/R). J.H.Z is grateful for the support of Millenium Project RC120001 of ICM.

References

[1] K. Nagpal, S.K. Singh, D.N. Mishra. *Chem. Pharm. Bull.*, **58**, 1423 (2010).
[2] J.J. Wang, Z.W. Zeng, R.Z. Xiao, T. Xie, G.L. Zhou, X.R. Zhan, S.L. Wang. *Int. J. Nanomed.*, **6**, 765 (2011).
[3] H.Y. Zhou, Y.P. Zhang, W.F. Zhang, X.G. Chen. *Carbohydr. Polym.*, **83**, 1643 (2011).
[4] Z. Guo, J. Ren, F. Dong, G. Wang, P. Li. *J. Appl. Polym. Sci.*, **127**, 2553 (2013).
[5] Y. Hu, Y. Du, J. Yang, J.F. Kennedy, X. Wang, L. Wang. *Carbohydr. Polym.*, **67**, 66 (2007).
[6] M. Kong, X.G. Chen, K. Xing, H.J. Park. *Int. J. Food Microbiol.*, **144**, 51 (2010).
[7] G.Q. Ying, W.-Y. Xiong, H. Wang, Y. Sun, H.-Z. Liu. *Carbohydr. Polym.*, **83**, 1787 (2011).
[8] J.E. Dos Santos, E.R. Dockal, E.T.G. Cavalheiro. *Carbohydr. Polym.*, **60**, 277 (2005).
[9] X.D. Shangguan, J.B. Zheng. *Electroanalysis*, **21**, 881 (2009).
[10] X.F. Zeng, E.J. Ruckenstein. *J. Membr. Sci.*, **148**, 195 (1998).
[11] M.S. Chiou, H.Y. Li. *J. Hazard. Mater.*, **93**, 233 (2002).
[12] E. Guibal, C. Milot, J.M. Tobin. *Ind. Eng. Chem. Res.*, **37**, 1454 (1998).
[13] J.R. Evans, W.G. Davids, J.D. MacRae, A. Amirbahman. *Water Res.*, **36**, 3219 (2002).
[14] W.S.W. Ngah, S.A. Ghani, L.L. Hoon. *J. Chin. Chem. Soc.-Taip.*, **49**, 625 (2002).
[15] A.-H. Chen, S.-Ch. Liu, C.-Y. Chen, C.-Y. Chen. *J. Hazard. Mater.*, **154**, 184 (2008).
[16] Y.C. Chang, D.H. Chen. *J. Colloid Interface Sci.*, **283**, 446 (2005).
[17] Y.C. Chang, D.H. Chen. *Macromol. Biosci.*, **5**, 254 (2005).
[18] Y.-C. Chang, S.-W. Chang, D.-H. Chen. *React. Funct. Polym.*, **66**, 335 (2006).
[19] H. Huang, N. Hu, Y. Zeng, G. Zhou. *Anal. Biochem.*, **308**, 141 (2002).
[20] L. Jiang, R. Wang, X. Li, L. Jiang, G. Lu. *Electrochem. Commun.*, **7**, 597 (2005).
[21] M.A. Gulppi, M.A. Paez, J.A. Costamagna, G. Cárdenas-Jirón, F. Bedioui, J.H. Zagal. *J. Electroanal. Chem.*, **580**, 50 (2005).

[22] G.I. Cárdenas-Jirón, M.A. Gulppi, C.A. Caro, R. del Río, M. Páez, J.H. Zagal. *Electrochim. Acta*, **46**, 3227 (2001).

[23] J.H. Zagal, M.A. Gulppi, C.A. Caro, G.I. Cárdenas-Jirón. *Electrochem. Commun.*, **1**, 389 (1999).

[24] C.A. Caro, G. Cabello, E. Landaeta, J. Pérez, J.H. Zagal, L. Lillo. *Russ. J. Appl. Chem.*, **86**, 1791 (2013).

[25] H.-P. Chang, H.-T. Yao, M.-T. Chiang. *J. Food Drug Anal.*, **20**, 661 (2012).

[26] J. Costamagna, L.E. Lillo, B. Matsuhiro, M.D. Noseda, M. Villagrán. *Carbohydr. Res.*, **338**, 1535 (2003).

[27] C.M. Da Silva, D.L. da Silva, L.V. Modolo, R.B. Alves, M.A. de Resende, C.V.B. Martins, Â. de Fátima. *J. Adv. Res.*, **2**, 1 (2011).

[28] L.E. Lillo, B. Matsuhiro. *Carbohydr. Polym.*, **34**, 397 (1997).

[29] J. Costamagna, L.E. Lillo, B. Matsuhiro, M. Villagrán. *Bol. Soc. Chil. Quím.*, **45**, 377 (2000).

[30] J. Costamagna, N.P. Barroso, B. Matsuhiro, M. Villagrán. *Inorg. Chim. Acta*, **273**, 191 (1998).

[31] J.H. Zagal, F.J. Recio, C.A. Gutierrez, C. Zuñiga, M.A. Páez, C.A. Caro. *Electrochem. Commun.*, **41**, 24 (2014).

[32] C.A. Caro, J.H. Zagal, F. Bedioui. *J. Electrochem. Soc.*, **150**, E95–E103 (2003).

[33] C. Hansch, A. Leo, R.W. Taft. *Chem. Rev.*, **91**, 165 (1991).

[34] D. Schlettwein, T. Yoshida. *J. Electroanal. Chem.*, **441**, 139 (1998).

[35] J.H. Zagal, M.A. Gulppi, G.I. Cárdenas-Jirón. *Polyhedron*, **19**, 2255 (2000).

[36] J.H. Zagal, G.I. Cárdenas-Jirón. *J. Electroanal. Chem.*, **489**, 96 (2000).